Journal of the Australian Ceramic Society (2022) 58:747–756
https://doi.org/10.1007/s41779-022-00718-1

RESEARCH

Ionizing radiation shielding efficiency and elastic properties of zirconium/cobalt/nickel/vanadium lithium borotellurite glasses

Y. S. Rammah[1] · E. M. Abou Hussein[2] · Shams H. Abdel-Hafez[3] · I. O. Olarinoye[4] · A. Gamal[1] · F. I. El-Agawany[1] · M. S. Shams[5]

Received: 8 May 2021 / Revised: 5 October 2021 / Accepted: 6 February 2022 / Published online: 25 March 2022

Abstract

The mechanical and radiation interaction parameters are vital for characterizing a material as potential shields in nuclear radiation protection applications. This study presents a glass system with the following formula: $56B_2O_3$-$25Li_2O_3$-$10Na_2O$-5CaO-$2Al_2O_3$-2SrO-$0.5TeO_2$-1X wt%: $X = ZrO_2$ (G1-Zr), CoO (G2-Co), NiO (G3-Ni), and V_2O_5 (G4-V). The photon attenuation parameters were evaluated through the use of XCOM software for typical photon energy sources used in medical and research applications of photons (22–1330 keV). In addition, the mechanical properties of glasses were examined. The maximum value of the mass attenuation coefficient (μ_m) of 2.356, 2.049, 2.073, and 1.958 cm^2/g for G1-Zr, G2-Co, G3-Ni, and G4-V, respectively, was obtained at the least energy of 22 keV. The minimum value of μ_m was obtained at 1.33 MeV with corresponding value of 0.054 cm^2/g for the four glasses. The range of effective atomic number (Z_{eff}) of the glasses was 7.189–17.88, 7.182–16.242, 7.185–16.353, and 7.171–15.869 for G1-Zr, G2-Co, G3-Ni, and G4-V, respectively, for the considered energy spectrum. Based on the half value layer (HVL) value at 662 keV, it is clear that the present glasses are better photon absorbers than OC and RS-253-G18 glass shield. The value of Σ_R for the glasses revealed that G4-V is a better fast neutron absorber among the investigated glasses. The G1-Zr glass sample has a minimum elastic moduli values, but G3-Ni sample has the maximum values. Generally, the investigated glasses can be used as appropriate materials for gamma-ray shielding applications.

Keywords Lithium borotellurite glasses · Photon · HVL · Elastic moduli

Introduction

In our present technologically advanced world, glasses are exhaustively being used in a wide variety of applications ranging from household appliances, optical, telecommunication and electronic devices, and so on [1–4]. Over the years, the scope of glass application continues to develop due to many interesting general properties of glass materials. One major factor that has sustained such development is the chemical compositional flexibility enjoyed by glass materials. The implication of this is that the chemical content of a glass can be varied easily to obtain a different glass composition. Since the general (mechanical, physical, structural, optical, etc.) properties of a glass material rest majorly on its chemical content, it is hence possible for new glass material having novel properties to emerge from existing ones [1–6]. This has led to the synthesis and characterization of different glass species for different applications. It has also produced new glasses with potential applications

✉ Y. S. Rammah
dr_yasser1974@yahoo.com

1 Department of Physics, Faculty of Science, Menoufia University, 32411 Shebin El-Kom 32511, Shibin El Kom, Egypt

2 Radiation Chemistry Department, National Center for Radiation Research and Technology, Atomic Energy Authority, P. O. Box 8029, Nasr City, Cairo 11371, Egypt

3 Department of Chemistry, College of Science, Taif University, P.O.Box 11099, Taif 21944, Saudi Arabia

4 Department of Physics, School of Physical Sciences, Federal University of Technology, Minna, Nigeria

5 Physics and Mathematical Engineering Department, Faculty of Electronic Engineering, Menoufia University, Menouf, Egypt

in emerging technologies outside the traditional sphere of glass use [6–13].

The earth and its inhabitants have continued to be irradiated from artificial radiation generators due to the enormous use of these sources in modern technology. As nuclear radiation technology continues to grow, so also are radiation control and protection measures, particularly in the areas of radiation shielding [6, 8–13]. The use of radiation barriers (shields) for the absorption and hence the reduction of radiation dose to man and his environment is a very crucial aspect of radiation technology. This is due to the deleterious effect of unhindered exposure of living and nonliving systems to ionizing radiation. Although the major factor to consider before a material can be adopted for radiation shield is its ability to effectively attenuate the radiation type, it is meant to shield to acceptable level; however, many other parameters such as availability, mechanical strength, physical properties, and stability are other characteristics to be considered. These secondary parameters dictate in what form (pure or infused with other materials) and the nature of environment suitable for such material to function effectively.

Environmental factors, stability, and economic concerns have placed restrictions on the use of some shielding materials such as Pb and Pb-based materials. Consequently, the synthesis and testing of environmentally friendly, cheap, and durable radiation shielding materials are very attractive to the research community. Some studies have focused on alloys, steel, metallic glasses, rocks/soil, glasses, and other types of materials for their shielding competence against gamma, neutrons, and charged particles [14–18]. Among these new generation of cheap and nontoxic shields, glasses have received more attention and outshine other materials in terms of ease of production, durability, optical transparency, and superior shielding competence [14–20]. Today, many glass samples have been produced with good potential for advance shielding applications.

The gamma radiation absorption competence of a glass material depends on the incident photon energy, atomic number, and proportion of the chemical elements in the glass matrix and its thickness. Recently, Aygun et al. [21] investigated photon and fast neutron absorption parameters of metal oxides doped glasses. The metal oxides considered in the study were CoO, $CdWO_4$, Bi_2O_3, Cr_2O_3, and Bi_2O_3. The research showed that photon and fast neutron shielding parameters of the doped glasses were affected by the molecular mass, density, and photon absorption capacity of the metal oxides. Similar observation has been reported for Sb_2O_3, PbF_2, and MoO_3 in different glass matrices [15, 20, 22]. The present study presents a glass system with the following formula: $56B_2O_3$-$25Li_2O_3$-$10Na_2O$-5CaO-$2Al_2O_3$-2SrO-$0.5TeO_2$-1X wt%: $X = ZrO_2$, CoO, NiO, and V_2O_5 and their photon and fast neutron absorption parameters. The photon attenuation parameters were calculated for typical photon energy sources used in medical and research applications of photons. In addition, the mechanical properties of glasses were examined.

Materials and methods

Materials

Four samples of lithium borotellurite glasses with the formula $56B_{2O3}$-$25Li_{2O3}$-$10Na_2O$-5CaO-$2Al_{2O3}$-2SrO-$0.5TeO_2$-1X wt%: $X = ZrO_2$, CoO, NiO, and V_{2O5} were selected from Ref. [23]. More details for the preparation steps and glasses' physical properties were written in [23]. The investigated glasses were named as follows:

G1-Zr: $56B_{2O3}$-$25Li_{2O3}$-$10Na_2O$-5CaO-$2Al_{2O3}$-2SrO-$0.5TeO_2$-$1ZrO_2$ wt%

G1-Co: $56B_{2O3}$-$25Li_{2O3}$-$10Na_2O$-5CaO-$2Al_{2O3}$-2SrO-$0.5TeO_2$-1CoO wt%

G1-Ni: $56B_{2O3}$-$25Li_{2O3}$-$10Na_2O$-5CaO-$2Al_{2O3}$-2SrO-$0.5TeO_2$-1NiO wt%

G1-V: $56B_{2O3}$-$25Li_{2O3}$-$10Na_2O$-5CaO-$2Al_{2O3}$-2SrO-$0.5TeO_2$-$1V_{2O5}$ wt%

Samples name, compositions, and density of investigated glasses are tabulated in Table 1.

Photon and neutron shielding parameters

The radiation attenuating and hence protection efficiency of a medium may be described using radiation interaction parameters. These parameters give the level of attenuation with respect to radiation type and energy. For photons, the mass attenuation coefficient μ_m describes the measure of photon intensity that transmits through a medium. Usually, μ_m depends on the absorber's chemical definition and energy of photon. For the present glasses (G1-Zr, G2-Co, G3-Ni, and G4-V), μ_m values for photon energy sources usually used in medical applications were calculated via the XCOM software [24]. Other gamma radiation interaction parameters that may be used to describe photon protection capacity include the following: the effective atomic number Z_{eff}, half-value layer/thickness (HVL), and mean free path (MFP), all of which are strongly dependent on the photon energy. Mathematically, these parameters were obtained directly from μ_m for the present glasses according to the following equations [25, 26]:

$$Z_{eff} = \frac{\sum_i f_i A_i (\mu_m)_i}{\sum_j f_j \frac{A_j}{Z_j} (\mu_m)_j}; MFP = {}^{1}\!/_{\rho\mu_m}; HVL = {}^{ln2}\!/_{\rho\mu_m} \quad (1)$$

Table 1 Sample's name, chemical composition, and density of $56B_{2O3}$-$25Li_{2O3}$-$10Na_2O$-5CaO-$2Al_{2O3}$-2SrO-$0.5TeO_2$-1X wt%: $X = ZrO_2$, CoO, NiO, and V_{2O5} glasses

Sample's name	Chemical composition (wt%)	X				Density, (g/cm^3)
	$B_2O_3/Li_2O_3/Na_2O/CaO/Al_2O_3/SrO/0TeO_2$	ZrO_2	CoO	NiO	V_2O_5	
G1-Zr	$56B_{2O3}/25Li_{2O3}/10Na_2O/5CaO/2Al_{2O3}/2SrO/0.5TeO$	1	0	0	0	2.299
G2-Co	$56B_{2O3}/25Li_{2O3}/10Na_2O/5CaO/2Al_{2O3}/2SrO/0.5TeO_2$	0	1	0	0	2.361
G3-Ni	$56B_{2O3}/25Li_{2O3}/10Na_2O/5CaO/2Al_{2O3}/2SrO/0.5TeO_2$	0	0	1	0	2.368
G4-V	$56B_{2O3}/25Li_{2O3}/10Na_2O/5CaO/2Al_{2O3}/2SrO/0.5TeO_2$	0	0	0	1	2.395

where f_i, Z_i, A_i, and ρ are the molar fraction, atomic number, and atomic mass number of the i^{th} elemental component and density of the absorbing glass.

Fast neutron shielding capacity of the glasses was assessed via the fast neutron removal cross section ($FNRC - \Sigma_R$). The *FNRC* measures the probability that a fast neutron interacting with a medium will be removed from the fast beam after its first collision. *FNRC* of the glasses were theoretically estimated via [27]: $\Sigma_R = \sum w_i(\frac{\Sigma_R}{\rho})_i$ where w_i, and $\left(\frac{\Sigma_R}{\rho}\right)_i$, is the density fraction and fast neutron mass removal cross section of the i^{th} element in the interacting material. Furthermore, $\frac{\Sigma_R}{\rho}$ was estimated according to [20, 28]:

$$\frac{\Sigma_R}{\rho} = 0.19Z^{-0.743} \text{for} 2 \le Z \le 8; \frac{\Sigma_R}{\rho} = 0.125Z^{-0.565} \text{for} Z > 8 \quad (2)$$

Elastic moduli of the investigated glasses

In order to evaluate the mechanical properties (bulk ($K_{B\text{-}C}$), shear ($S_{B\text{-}C}$), longitudinal ($L_{B\text{-}C}$), Young's ($E_{B\text{-}C}$)), and Poisson's ratio ($\sigma_{B\text{-}C}$) of the investigated lithium borotellurite glasses, the bond compression (B-C) model was applied [22, 29, 30]. All physical parameters and relations used for this aim were collected in Tables 2 and 3.

Results and discussion

Photon interaction parameters

The value of μ_m at different source energies is pictorially represented in Fig. 1. The figure shows that μ_m decays in value as energy (E) increases. However, the decay was rapid for each of the glasses at the lower end of the energy spectrum compared to the later end. The maximum value of the mass attenuation coefficient of 2.356, 2.049, 2.073, and 1.958 cm^2/g for G1-Zr, G2-Co, G3-Ni, and G4-V, respectively, was obtained at the least energy of 22 keV. The smallest value of μ_m was obtained at 1.33 MeV with corresponding value of 0.054 cm^2/g for the four glasses. The observed changes in the μ_m values within the E spectrum considered can be attributed to the changes in the partial photon absorption coefficients with respect to E. Within the investigated energy spectrum considered in this study, photoelectric (PEAC) and Compton scattering (CSAC) absorption coefficients are the major interaction cross sections dictating the behavior of μ_m. The PEAC and CSAC vary inversely as the 4th and 1st power of photon energy, respectively. The PEAC dominates μ_m at E less than 662 keV, while CSAC dominates proceeding for the rest of the energy spectrum. Value of μ_m at each energy increases according to the trend: $(\mu_m)_{G1\text{-}Zr} > (\mu_m)_{G3\text{-}Ni} > (\mu_m)_{G2\text{-}Co} > (\mu_m)_{G4\text{-}V}$. Obviously, this trend is influenced by the atomic weight and density of the doping elements (Zr, Co, Ni, and V). Heavier elements are known to be better photon absorbers due to their higher density and atomic number per unit mass. Consequently, the photon absorption capacity of

Table 2 Coordination number per cation (n_f), crosslink density per cation (n_c), stretching force constant (F), and ionic radius (r) of the oxides B_{2O3}, Li_{2O3}, Na_2O, CaO, Al_{2O3}, SrO, TeO_2, ZrO_2, CoO, NiO, V_{2O5}

Oxides	B_2O_3	Li_2O_3	Na_2O	CaO	Al_2O_3	SrO	TeO_2	ZrO_2	CoO	NiO	V_2O_5
n_f	3	4	4	6	4	6	4	6	4	6	5
n_c	1	2	2	4	2	4	2	4	2	4	3
F (N/m)	660	243	225	194.75	313.4	117.02	216	306.57	144	191.66	277
r (nm)	0.138	0.159	0.196	0.2059	0.1757	0.244	0.199	0.177	0.2277	0.207	0.196

Table 3 The values of total number of cationic per glass formula unit (η), average crosslink density ($\overline{n}_c$), average stretching force constant ($\overline{F}$), number of network bond per unit volume (n_b), average bond length (l), calculated bond compression elastic moduli (bulk ($K_{B\text{-}C}$), shear ($S_{B\text{-}C}$), longitudinal ($L_{B\text{-}C}$), Young's ($E_{B\text{-}C}$)), and Poisson's ratio ($\sigma_{B\text{-}C}$) of the investigated glasses

Parameters and elastic moduli	G1-Zr	G2-Co	G3-Ni	G4-V
$\eta \pm 0.001$	1.916	1.913	1.916	1.926
$\overline{\eta} = \frac{1}{\eta}\sum x_i (n_c)_i (N_c)_i \ \pm 0.001$	0.838	0.827	0.838	0.828
$\overline{F} = \frac{\sum (xn_f f)_i}{\sum (xn_f)_i} (N/m) \ \pm 0.001$	426.790	425.664	424.906	426.719
$n_b = \frac{N_A}{V_m}\sum (n_f x)_i \times 10^{28} (m^{-3}) \ \pm 0.001$	7.280	7.487	7.551	7.500
$l = \left(0.0106 \frac{\overline{F}}{K_{B-C}}\right)^{0.26} (nm) \ \pm 0.001$	0.465	0.460	0.460	0.461
$K_{B-C} = \frac{N_A}{9V_m}\sum_i \left(n_f x \overline{F} r^2\right) (GPa) \pm 0.001$	85.939	88.870	89.151	88.769
$S_{B-C} = \left(\frac{3}{2}\right) K_{B-C} \left(\frac{1-2\sigma_{B-C}}{1+\sigma_{B-C}}\right) (GPa) \pm 0.001$	41.356	42.551	42.902	42.521
$L_{B-C} = K_{B-C} + \frac{4}{3} S_{B-C} (GPa) \pm 0.001$	140.943	145.463	146.211	145.322
$E_{B-C} = 2S_{B-C}(1 + \sigma_{B-C}) (GPa) \pm 0.001$	106.919	110.084	110.915	110.000
$\sigma_{B-C} = 0.28 (\overline{n}_c)^{-0.25} \pm 0.001$	0.292	0.293	0.292	0.293

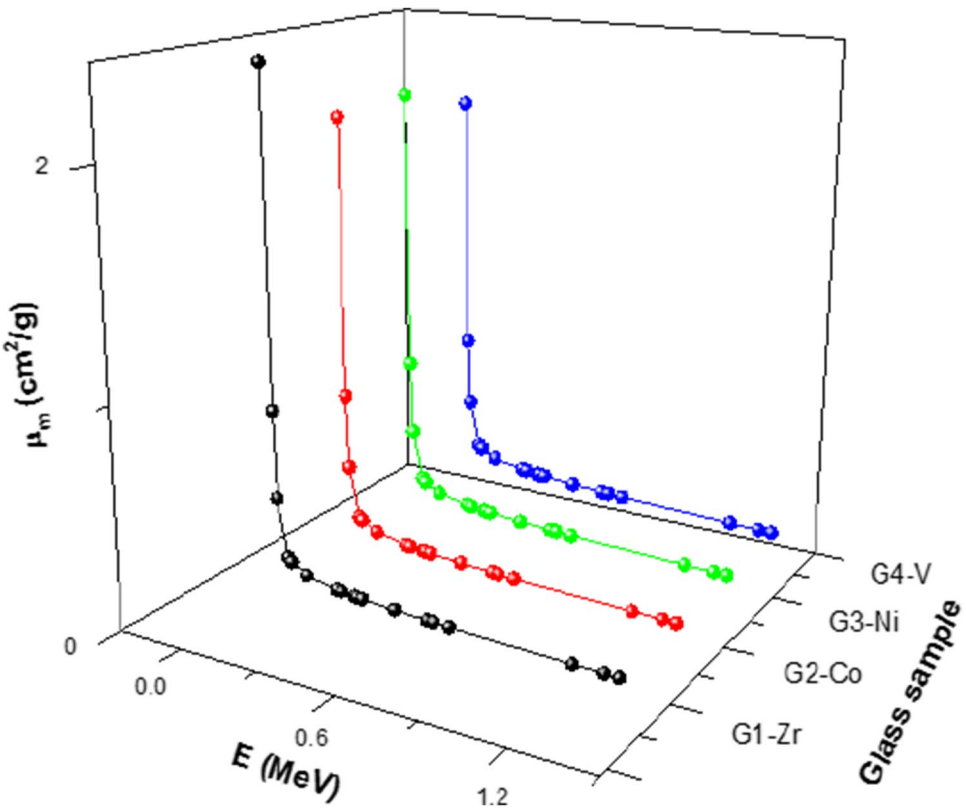

Fig. 1 Mass attenuation coefficient as a function of photon energy E of the investigated glasses

the glass system is improved by doping with heavy atomic species.

The consequence of the chemical composition on the two major interaction modes is made apparent in the photon interaction-induced effective atomic number Z_{eff}. Variations in the value of Z_{eff} with regard to photon energy for the glasses are portrayed in Fig. 2. The Z_{eff} spectra of the four glasses look similar: decreasing as E increases for each glass. This change is similar to that of mass attenuation coefficient of the glasses as predicted by PEAC and CSAC dependence on E. The PEAC depends on the 4th power of Z_{eff}; hence, the glass with higher cross sections for these interaction process possesses the highest effective atomic number. The range of Z_{eff} of the glasses was 7.189–17.88, 7.182–16.242, 7.185–16.353, and 7.171–15.869 for G1-Zr, G2-Co, G3-Ni, and G4-V, respectively, for the considered energy spectrum. Similar to μ_m, the value and range of the effective atomic number are strongly influenced by the atomic number of the

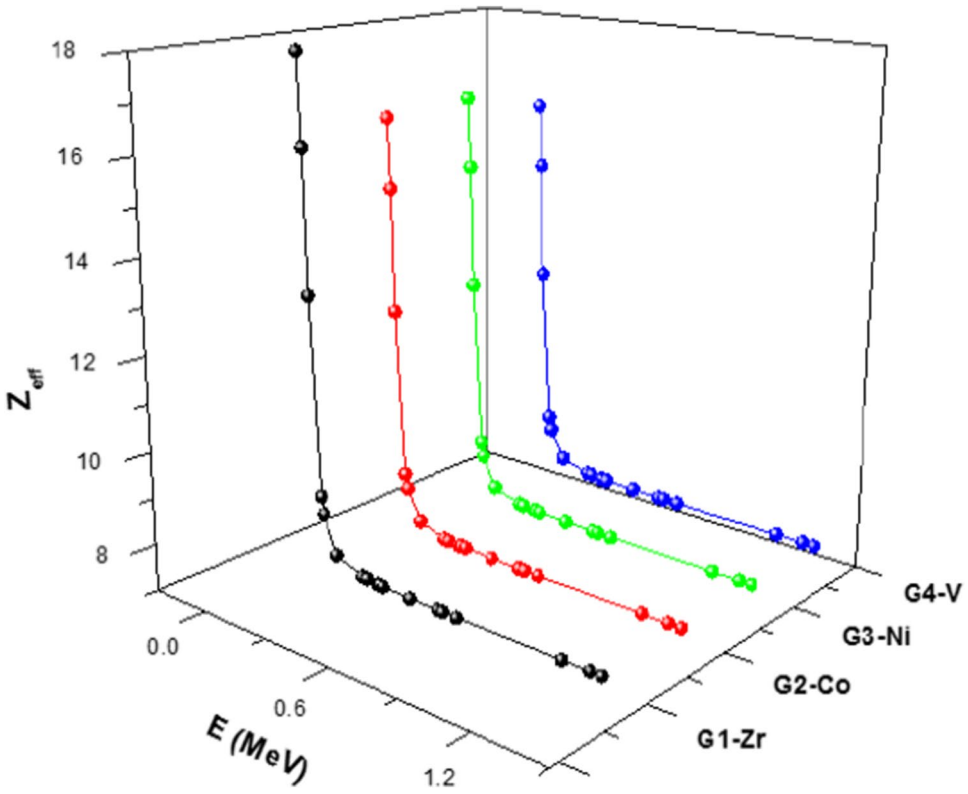

Fig. 2 Variation of Z_{eff} with E for the investigated glasses

dopant atomic number [25]. The similar trend in the value of Z_{eff} and μ_m implies that either parameters could be used to characterize the relative photon absorption capacity of the glasses.

The mean free path (MFP) of photon is the mean distance moved by a photon between interactions. It is a parameter that can also be used to compare photon absorption in different interacting media. Similar to other photon interaction parameters, MFP is energy dependent; its energy dependence for the investigated glass is shown in Fig. 3. The figure also shows the dopant atom dependence on the MFP. The MFP increases with energy; higher energy photons interact

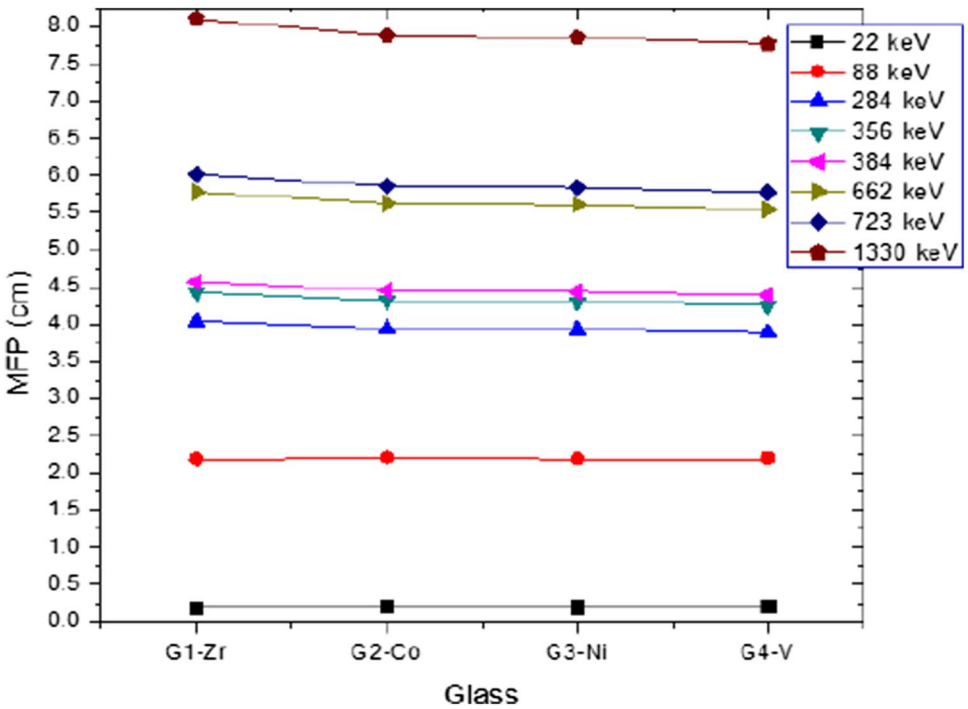

Fig. 3 Effect of dopant atom on the MFP of the glasses at different photon energy

less with absorber due to dwindling photon interaction cross sections. At lower energies, MFP is lower for the higher Z_{eff} glasses; however, as energy increases, the effect is reversed. The dominance of the CSAC is responsible for this reversed behavior. The CSAC depends on the number of electron per unit mass, a quantity which decreases with Z_{eff}. The HVL is a useful parameter which is always used to compare the photon shielding capacity of different absorbers. It defines the thickness of the glass material required to reduce photon intensity by 50%. The variation of HVL of the glasses with energy relative to those of ordinary concrete (OC) [31] and a commercial glass shields (RS-360 and RS-253-G18) [32] at 662 keV is depicted in Fig. 4. Based on the HVL value at 662 keV, it is clear that the present glasses are better photon absorbers than OC and RS-253-G18 glass shield.

Fast neutron macroscopic removal cross section (FNRCS, Σ_R)

The values of calculated Σ_R of the glasses are depicted pictorially in Fig. 5a. The Σ_R values varied from 0.1006 to 0.105 cm^{-1} for the glasses. There is a gradual growth in the FNRCS of the glasses which seems to be in consonance with the quantity of the partial Σ_R of Li and B atoms (Fig. 5b). As the dopant atomic species changes, it alters the atomic distribution of the chemical composition of the glasses. These alterations result in the increase in the partial density and Σ_R of the two mentioned atoms; their relatively higher fast neutron mass removal cross sections buttress this point. These two atomic species thermalize fast neutron via elastic interaction with the fast neutrons better than the other atoms in the glasses. Hence, the observed trend in the fast neutron moderating capacity of the glasses is as dictated by the Li and B weight content of the glasses. The value of Σ_R for the glasses revealed that G4-V is a better fast neutron absorber among the investigated glasses. Comparing the Σ_R of the present glasses with those of recently studied glasses (S30 (0.0506 cm^{-1}) and TVM60 (0.1055 cm^{-1}) [22, 33], graphite (FNRC = 0.077 cm^{-1}), and OC (FNRC = 0.094 cm^{-1}) [31], it is obvious that the fast neutron absorbing capacity of the G4-V glass is comparable to that of TVM60 but superior to those of OC, S30, and graphite.

Elastic moduli

The coordination number per cation (n_f), crosslink density per cation (n_c), stretching force constant (F), and ionic radius (r) of the oxides B_{2O3}, Li_{2O3}, Na_2O, CaO, Al_{2O3}, SrO, TeO_2, ZrO_2, CoO, NiO, and V_{2O5} are listed in Table 2. The values of total number of cationic per glass formula unit (η), average stretching force constant ($\overline{F}$), average crosslink density ($\overline{n}_c$), average bond length (l), and number of network bond per unit volume (n_b) for each glass sample were calculated and tabulated in Table 3. The elastic moduli (bulk ($K_{B\text{-}C}$),

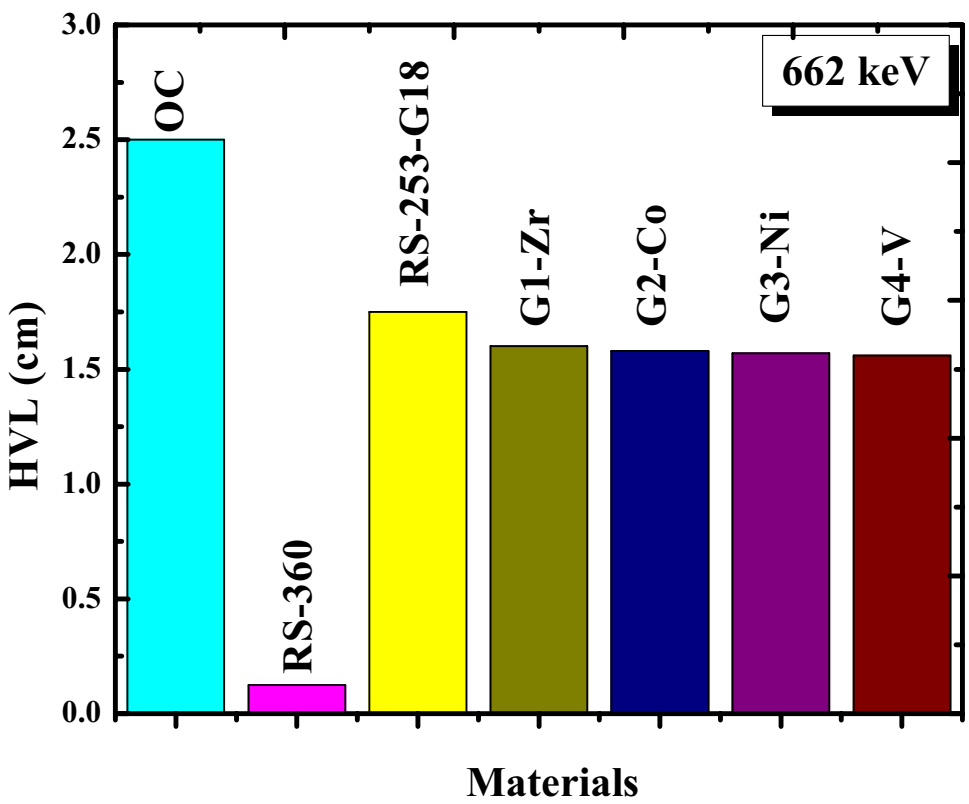

Fig. 4 Comparison of HVL of the glasses with some commercial shielding materials

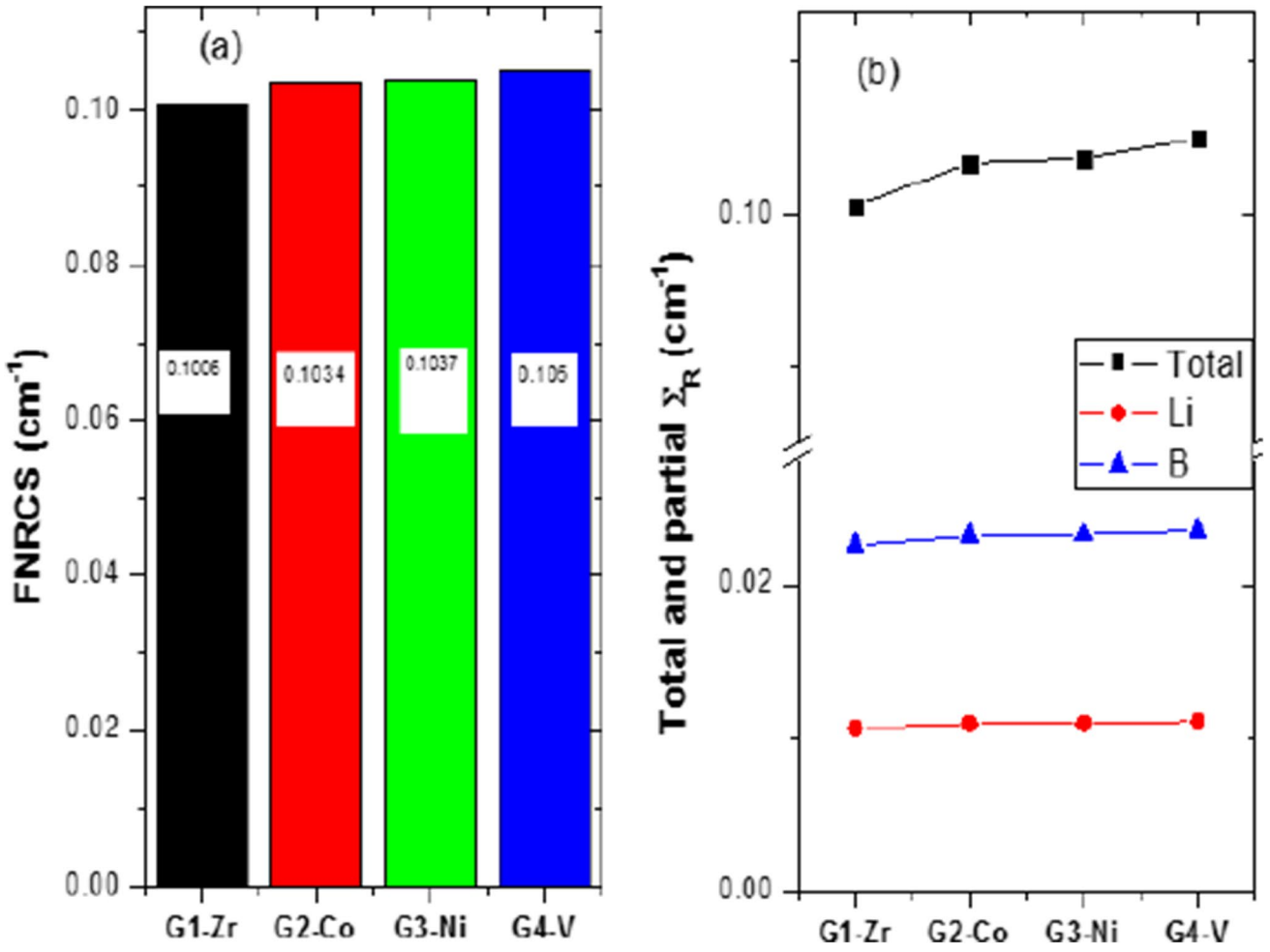

Fig. 5 **a** FNRCS and **b** total and partial Σ_R of the investigated glasses

shear ($S_{B\text{-}C}$), longitudinal ($L_{B\text{-}C}$), Young's ($E_{B\text{-}C}$)), and Poisson's ratio ($\sigma_{B\text{-}C}$) of BTLBB-glasses are evaluated and gathered in Table 3 and plotted as in Fig. 6. Results revealed that the elastic properties of the investigated glasses were slightly changed with changing the doping in the network structure. The calculated values of ($K_{B\text{-}C}$) were varied from 85.939 GPa for G1-Zr glass sample to 89.151 GPa for G3-Ni, ($E_{B\text{-}C}$) were varied from 106.919 GPa for G1-Zr glass sample to 110.915 GPa for G3-Ni sample, ($L_{B\text{-}C}$) were varied from 140.943 GPa G1-Zr glass sample to 145.463 GPa for G3-Ni sample, and ($S_{B\text{-}C}$) were changed from 41.356 GPa G1-Zr glass sample to 42.902 GPa for G3-Ni sample. These observations concluded that the G1-Zr glass sample has minimum elastic moduli values, but G3-Ni sample has the maximum values.

Figure 7 depicts the variation of Poisson's ratio ($\sigma_{B\text{-}C}$) and the average bond length (l) of the investigated glasses. The values of ($\sigma_{B\text{-}C}$) were fixed around 0.292, while the values of (l) were 0.465 (G1-Zr), 0.460 (G2-Co and G3-Ni), and 0.461 (G4-V).

Conclusion

This study presents a glass system with the following formula: $56B_{2O3}$-$25Li_{2O3}$-$10Na_2O$-5CaO-$2Al_{2O3}$-2SrO-$0.5TeO_2$-1X wt%: $X = ZrO_2$ (G1-Zr), CoO (G2-Co), NiO (G3-Ni), and V_{2O5} (G4-V). The photon attenuation parameters were calculated for typical photon energy sources used in medical and research applications of photons. Indeed, the mechanical properties of glasses were examined. Results revealed that the maximum value of the mass attenuation coefficient of 2.356, 2.049, 2.073, and 1.958 cm^2/g for G1-Zr, G2-Co, G3-Ni, and G4-V, respectively, was obtained at the least energy of 22 keV. The smallest value of μ_m was obtained at 1.33 MeV with corresponding value of 0.054 cm^2/g for the four glasses. The range of Z_{eff} of the glasses was 7.189–17.88, 7.182–16.242, 7.185–16.353, and 7.171–15.869 for G1-Zr, G2-Co, G3-Ni, and G4-V, respectively, for the considered energy spectrum. Based on the HVL value at 662 keV, it is clear that the present glasses are better photon absorbers than OC and RS-253-G18 glass

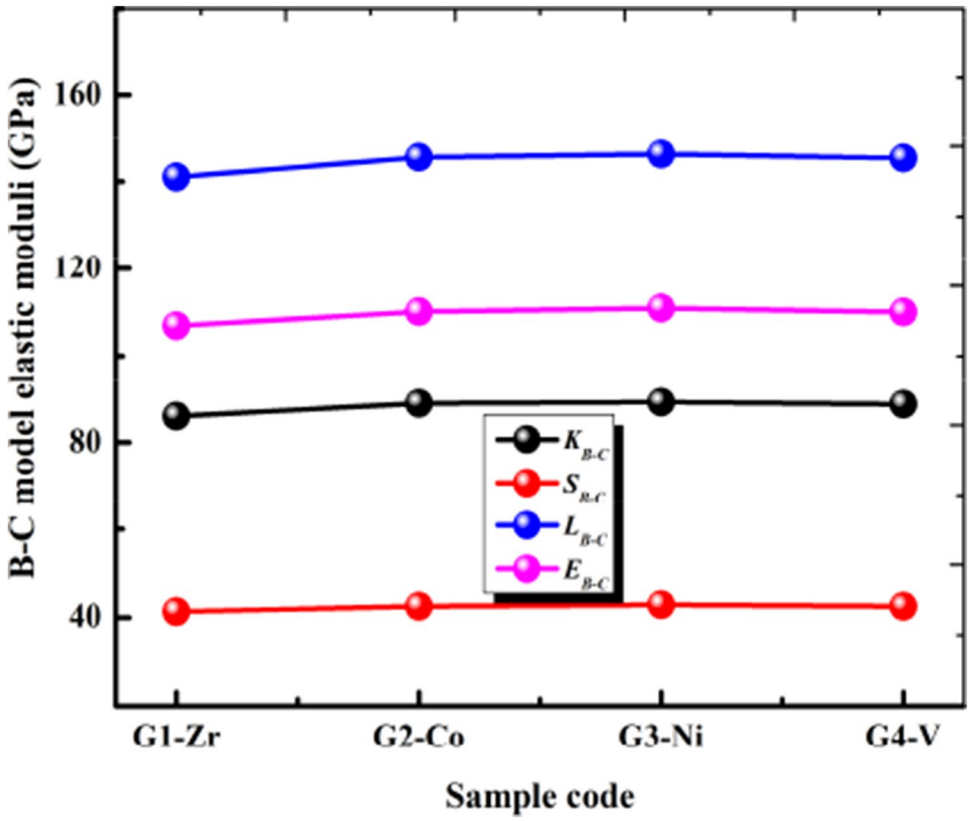

Fig. 6 B-C model elastic moduli of the investigated glasses

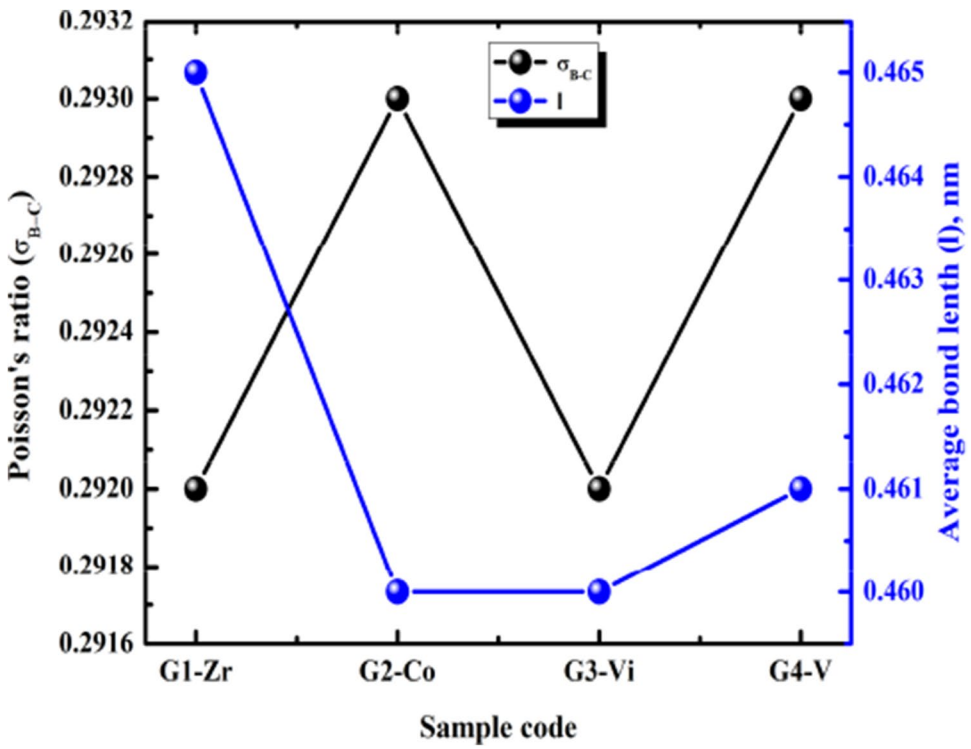

Fig. 7 Variation of Poisson's ratio and average bond length of the investigated glasses

shield. The value of Σ_R for the glasses revealed that G4-V is a better fast neutron absorber among the investigated glasses. The G1-Zr glass sample has a minimum elastic moduli values, but G3-Ni sample has the maximum values. Generally, the investigated glasses can be used as appropriate materials for gamma-ray shielding applications.

Acknowledgements Taif University Researchers Supporting Project number (TURSP-2020/23), Taif University, Taif, Saudi Arabia

Declarations

Conflict of interest The authors declare no competing interests.

References

1. Matori, K.A., Zaid, M.H.M., Aziz, S.H.A., Kamari, H.M., Wahab, Z.A.: Study of the elastic properties of (PbO)x(P2O5)1–x lead phosphate glass using an ultrasonic technique. J. Non-Cryst. Solids **361**, 78–81 (2013)
2. Laopaiboon, R., Bootjomchai, C.: Glass structure responses to gamma irradiation using infrared absorption spectroscopy and ultrasonic techniques: a comparative study between Co_{2O3} and Fe_{2O3}. Appl. Radiat. Isot. **89**, 42–46 (2014)
3. ElBatal, F.H., Abdelghany, A.M., ElBatal, H.A.: Characterization by combined optical and FT infrared spectra of 3d-transition metal ions doped-bismuth silicate glasses and effects of gamma irradiation. Spectrochim. Acta Part A Mol. Biomol. Spectrosc. **122**, 461–468 (2014). https://doi.org/10.1016/j.saa.2013.11.011
4. El-Batal, F.H., Khalil, E.M., Hamdy, Y.M., et al.: FTIR spectral analysis of corrosion mechanisms in soda lime silica glasses doped with transition metal oxides. SILICON **2**, 41–47 (2010). https://doi.org/10.1007/s12633-010-9037-8
5. Elazoumi, S.H., Sidek, H.A.A., Rammah, Y.S., El-Mallawany, R., Halimah, M.K., Matori, K., Zaid, M.H.M.: Effect of PbO on optical properties of tellurite glass. Results in Physics **8**, 16–25 (2018)
6. Y.S. Rammah, F.I. El-Agwany, K.A. Mahmoud, A. Novatski, R. El-Mallawany, Role of ZnO on TeO_2. Li_2O. ZnO glasses for optical and nuclear radiation shielding applications utilizing MCNP5 simulations and WinXCOM program. Journal of Non-Crystalline Solids, 544 (2020) 120162.
7. Ali, A.A., Rammah, Y.S., Shaaban, M.H.: The influence of TiO_2 on structural, physical and optical properties of B_{2O3} –TeO_2 – Na_2O – CaO glasses. J. Non-Cryst. Solids **514**, 52–59 (2019)
8. Y.S. Rammah, Gökhan Kilic, R. El-Mallawany, U. Gökhan Issever, F.I. El-Agawany, Investigation of optical, physical, and gamma-ray shielding features of novel vanadyl boro-phosphate glasses. Journal of Non-Crystalline Solids 533 (2020) 119905.
9. Sayyed, M.I., El-Mesady, I.A., Abouhaswa, A.S., Askin, A., Rammah, Y.S.: Comprehensive study on the structural, optical, physical and gamma photon shielding features of B_{2O3}-Bi_{2O3}-PbO-TiO_2 glasses using WinXCOM and Geant4 code. J. Mol. Struct. **1197**, 656–665 (2019)
10. Sayyed, M.I.: Bismuth modified shielding properties of zinc borotellurite glasses. J. Alloy. Compd. **688**, 111–117 (2016)
11. El-Bashir, B.O., Sayyed, M.I., Zaid, M.H.M., Matori, K.A.: Comprehensive study on physical, elastic and shielding properties of ternary BaO-Bi_{2O3}-P_{2O5} glasses as a potent radiation shielding material. J. Non-Cryst. Solids **468**, 92–99 (2017)
12. Sayyed, M.I., Kaky, K.M., Gaikwad, D.K., Agar, O., Gawai, U.P., Baki, S.O.: Physical, structural, optical and gamma radiation shielding properties of borate glasses containing heavy metals (Bi_{2O3}/MoO_3). J. Non-Cryst. Solids **507**, 30–37 (2019)
13. Issa, S.A., Tekin, H.O., Elsaman, R., Kilicoglu, O., Saddeek, Y.B., Sayyed, M.I.: Radiation shielding and mechanical properties of Al_{2O3}-Na_2O-B_{2O3}-Bi_{2O3} glasses using MCNPX Monte Carlo code. Mater. Chem. Phys. **223**, 209–219 (2019)
14. E. Sakar, Determination of photon-shielding features and build-up factors of nickel–silver alloys. Radiat. Phys. Chem 172 (2020) 108778.
15. Rammah, Y.S., Olarinoye, I.O., El-Agawany, F.I., El-Adawy, A.: The impact of PbF_2 on the ionizing radiation shielding competence and mechanical properties of TeO_2–PbF2 glasses and glass-ceramics. Ceram. Int. **47**, 2547–2556 (2021)
16. S.O. Araz, G. Hasan, U.B. Bayca, A. Abdullah, Investigation of gamma-ray attenuation coefficients for solid boronized 304L stainless steel, Appl Radiat Isot (2021) 109605.
17. O. Olarinoye, O. Celestine, Gamma-rays and fast neutrons shielding parameters of two new Ti-based bulk metallic glasses, Iran J Med Phys (2020).
18. Eke, C.: Investigation of gamma-ray attenuation properties of beach sand samples from Antalya, Turkey. Arab. J. Geosci. **14**, 1–16 (2021)
19. Zaid, M. H. M., H. A. A. Sidek, K. A. Matori, A. Abdu, K. A. Mahmoud, Maha M. Al-Shammari, E. Lacomme, Mohammad A. Imheidat, M. I. Sayyed, Influence of heavy metal oxides to the mechanical and radiation shielding properties of borate and silica glass system, J Mater Res Technol 11 (2021) 1322–1330.
20. M.S. Al-Buriahi, H.H. Hegazy, F. Alresheedi, H. H. Somaily, C. Sriwunkum, I. O. Olarinoye Effect of Sb_{2O3} addition on radiation attenuation properties of tellurite glasses containing V_{2O5} and Nb_{2O5}, Appl. Phys. A 127 (2021) 106.
21. Aygün, Bünyamin, Erdem Şakar, Esra Cinan, Nergiz Yıldız Yorgun, M. I. Sayyed, O. Agar, and Abdulhalik Karabulut, Development and production of metal oxide doped glasses for gamma ray and fast neutron shielding, Radiat Phys Chem 174 (2020) 108897.
22. I.O. Olarinoye, F.I. El-Agawany, A. El-Adawy, El Sayed Yousef, Y.S. Rammah, Mechanical features, alpha particles, photon, proton, and neutron interaction parameters of TeO_2–V_{2O3}–MoO_3 semiconductor glasses, Ceram Int 46 (2020) 23134–23144.
23. E.M. Abou Hussein, N.A. El-Alaily, Study on the effect of gamma radiation on some spectroscopic and electrical properties of lithium borate glasses, J Inorgan Organometal Polymers Mater 28 (2018) 1214–1225.
24. Gerward, L., Guilbert, N., Jensen, K.B., Levring, H.: WinXCom - a program for calculating X-ray attenuation coefficients. Radiat. Phys. Chem. **71**, 653–654 (2004)
25. Olarinoye, I.: Variation of effective atomic numbers of some thermoluminescence and phantom materials with photon energies. Res J Chem Sci **1**(2), 64–69 (2011)
26. Y.S. Rammah, M.I. Sayyed, A.A. Ali, Tekin, H.O., R. El-Mallawany, Optical properties and gamma shielding features of bismuth borate glasses. Appl Phys A124 (2018) 824–832.
27. El-Khayatt, A.: Calculation of fast neutron removal cross-sections for some compounds and materials. Ann. Nucl. Energy **37**(2), 218–222 (2010)
28. El-Abd, A., Mesbah, G., Mohammed, N.M.A., Ellithi, A.: A simple method for determining the effective removal cross section for fast neutrons. J. Radiatiot. Nucl. Appl. **2**, 53–85 (2016)
29. Y.S. Rammah, I.O. Olarinoye, F.I. El-Agawany, A. El-Adawy, A. Gamal, El Sayed Yousef., Elastic moduli, photon, neutron, and proton shielding parameters of tellurite bismo-vanadate (TeO_2–V_{2O5}–Bi_{2O3}) semiconductor glasses, Ceram Int 46 (2020) 25440–25452.

30. N. Elkhoshkhany, E. Syala, E. Yousef, Concentration dependence of the elastic moduli, thermal properties, and non-isothermal kinetic parameters of Yb^{3+} doped multicomponent tellurite glass system, Res Phys 16 (2020) 102876.
31. Bashter, I.I.: Calculation of radiation attenuation coefficients for shielding concretes. Ann. Nucl. Energy **24**(17), 1389–1401 (1997)
32. SCHOTT commercial glasses. A.G. Schott, http://www.schott.com/advanced optics/ English/products/opticalmate- rials/special materials/radiation-shielding-glasses/index.html.
33. Perişanoğlu, U., El-Agawany, F.I., Kavaz, E., Al-Buriahi, M., Rammah, Y.S.: Surveying of Na2O3–BaO–PbO–Nb2O5–SiO2–Al2O3 glass-ceramics system in terms of alpha, proton, neutron and gamma protection features by utilizing GEANT4 simulation codes. Ceram. Int. **46**, 3190–3202 (2020)